Supporting Information

In-situ decorate Ni_2P nanocrystals co-catalysts on g-C_3N_4 for efficient and stable photocatalytic hydrogen evolution via a facile co-heating method

Peng Wen[a‡], Kefei Zhao[a‡], Hui Li[b‡], Jiangsheng Li[c], Jing Li[a], Qing Ma[d], Scott M Geyer[b*], Lin Jiang[e*] and Yejun Qiu[a*]

[a]*Shenzhen Engineering Lab of Flexible Transparent Conductive Films, School of Materials Science and Engineering, Harbin Institute of Technology, Shenzhen, 518055, China. E-mail: yejunqiu@hit.edu.cn*

[b]*Department of Chemistry, Wake Forest University, Winston-Salem, North Carolina 27109, United States. E-mail: geyersm@wfu.edu*

[c]*School of Chemistry and Food Engineering, Changsha University of Science & Technology, Changsha 410114, China*

[d]*Teaching Center for Experimentation and Innovation Practice, Harbin Institute of Technology, Shenzhen, 518055, China*

[e]*Institute of Functional Nano & Soft Materials Laboratory (FUNSOM), Jiangsu Key Laboratory for Carbon-Based Functional Materials & Devices, Soochow University, Suzhou 215123, China. E-mail: ljiang@suda.edu.cn*

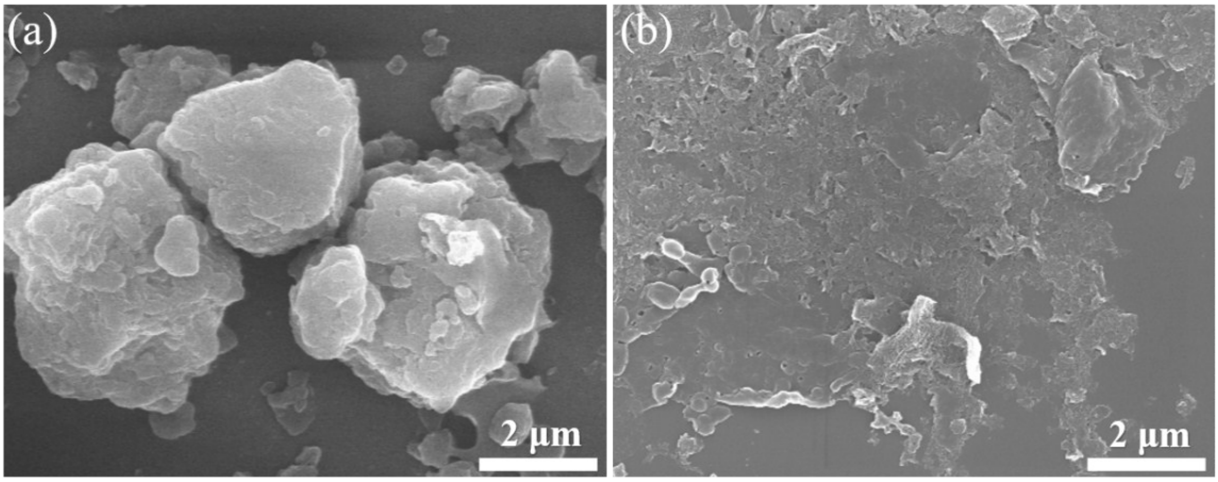

Fig. S1 SEM images of (a) bulk g-C_3N_4 and (b) g-C_3N_4 nanosheets.

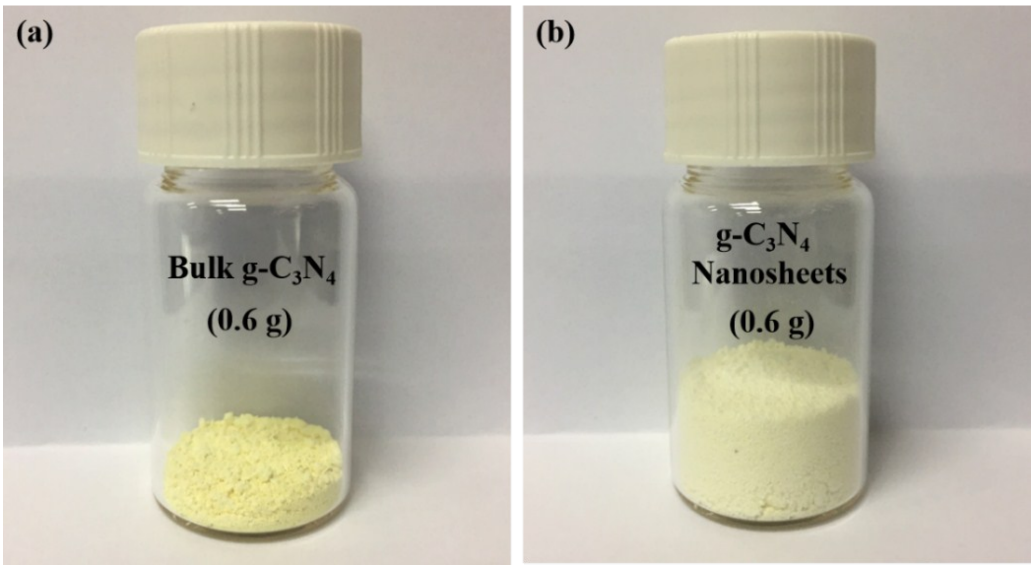

Fig. S2 Digital photographs of (a) bulk g-C_3N_4 and (b) g-C_3N_4 nanosheets.

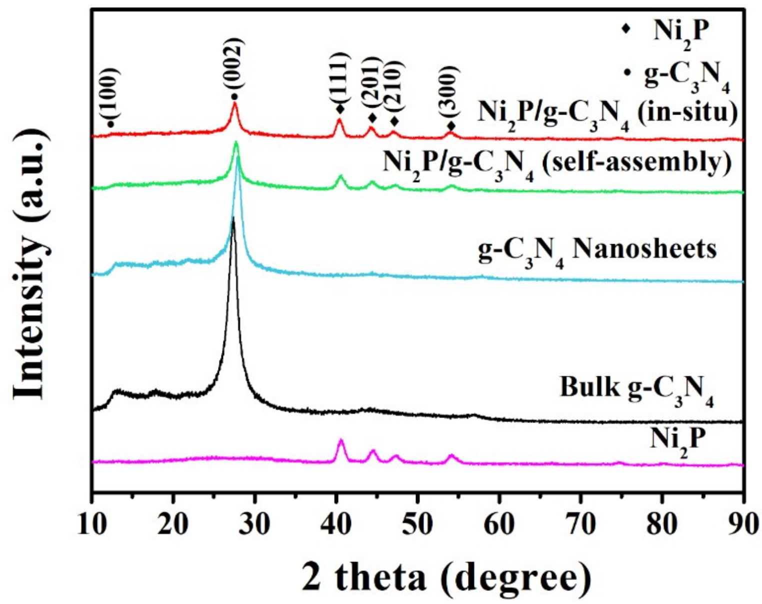

Fig. S3 XRD patterns of pure Ni_2P, bulk g-C_3N_4, g-C_3N_4 nanosheets and Ni_2P/g-C_3N_4 (self-assembly and in-situ) samples.

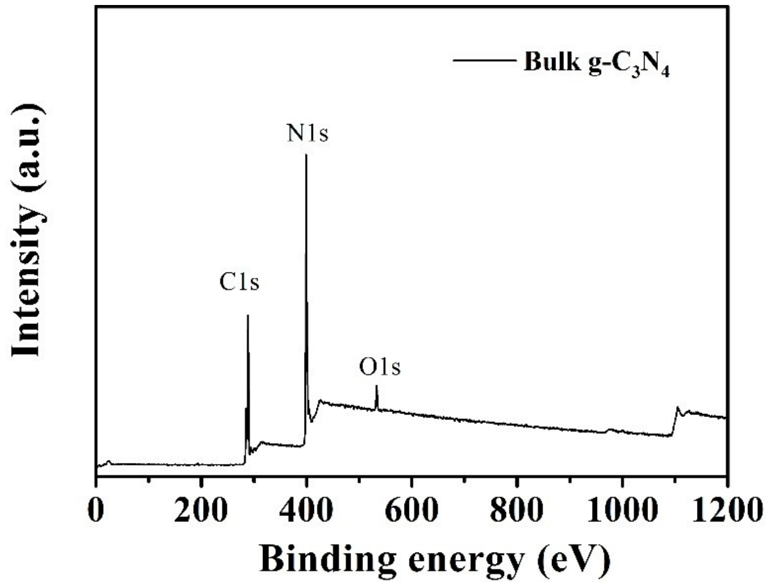

Fig. S4 XPS survey spectra of bulk g-C_3N_4 sample.

Table S1

The atomic percent of C, N, and O in bulk g-C_3N_4 sample.

Element	C	N	O
Atomic (%)	42.74	54.18	3.08
Calcd wt (%)	38.83	57.44	3.73

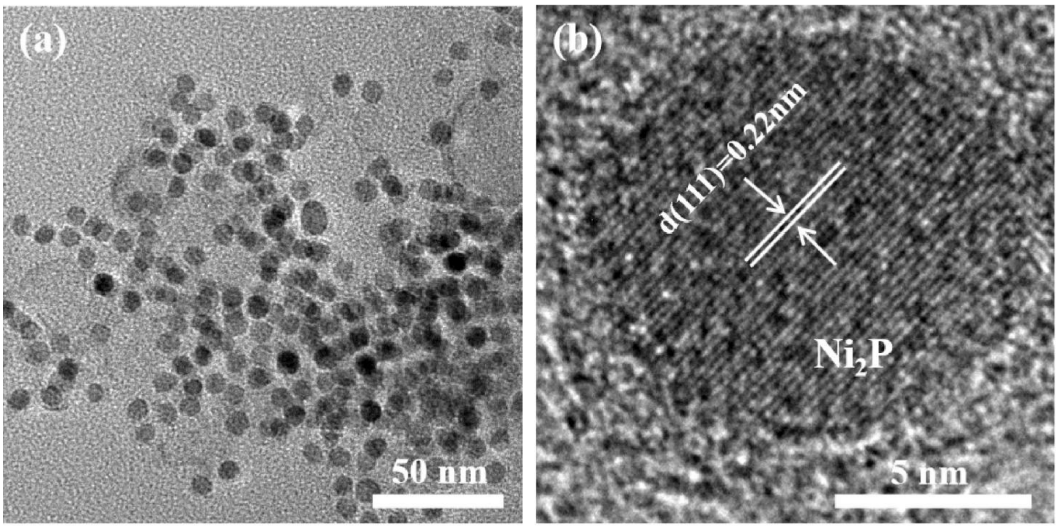

Fig. S5 (a) TEM and (b) HRTEM images of Ni_2P nanocrystals.

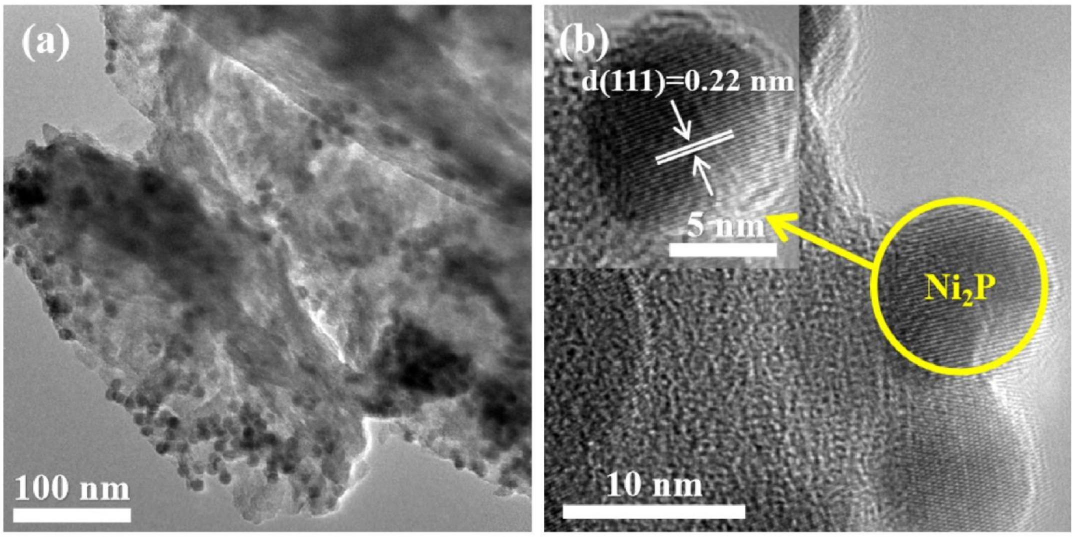

Fig. S6 (a) TEM and (b) HRTEM images of g-C_3N_4/Ni_2P composite prepared by self-assembly method.

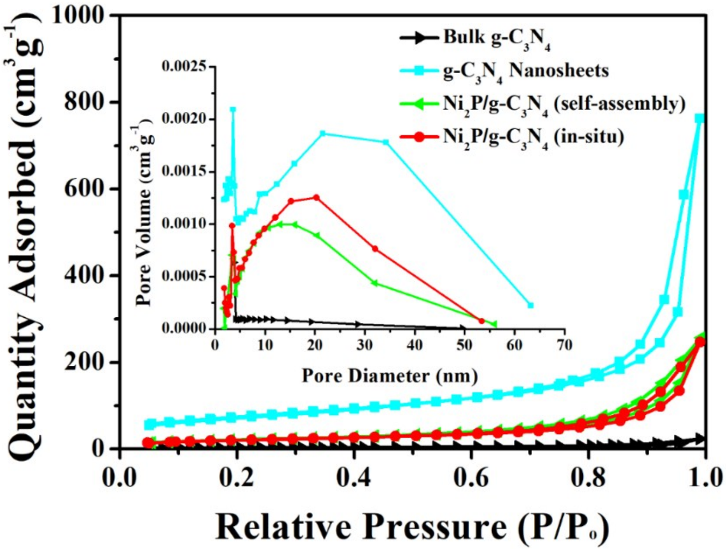

Fig. S7 N_2 adsorption-desorption isotherms and pore diameter distributions (inset) of bulk g-C_3N_4, g-C_3N_4 NSs and Ni_2P/g-C_3N_4 (self-assembly and in-situ) samples.

Table S2 Specific surface area, pore volumes and pore diameters of the prepared samples.

Sample	**S_{BET}/m^2 g^{-1}**	**V_{pore}/cm^3 g^{-1}**	**d_{pore}/nm**
Bulk g-C_3N_4	9.7	0.04	14.3
g-C_3N_4 Nanosheets	260.3	1.17	19.9
Ni_2P/g-C_3N_4 (self-assembly)	78.3	0.39	17.7
Ni_2P/g-C_3N_4 (in-situ)	74.9	0.38	19.2

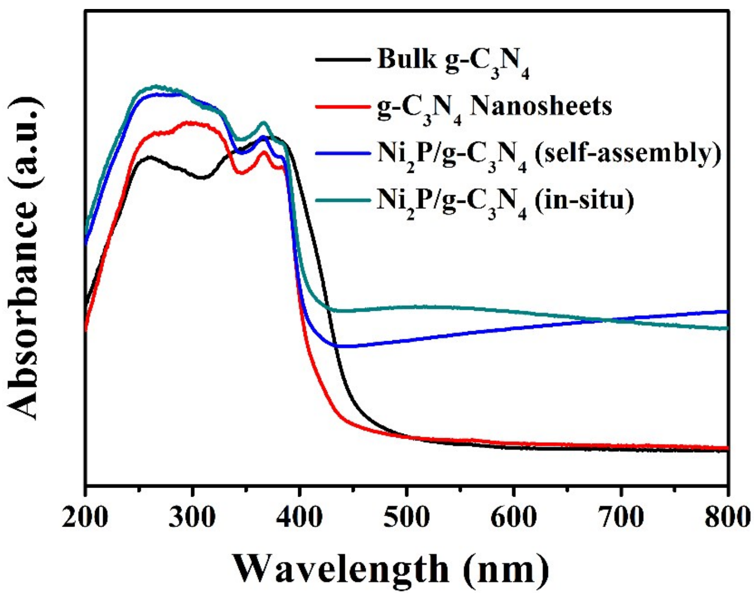

Fig. S8 UV-vis absorption spectra of bulk g-C_3N_4, g-C_3N_4 nanosheets, Ni_2P/g-C_3N_4 (in-situ) and Ni_2P/g-C_3N_4 (self-assembly) samples.

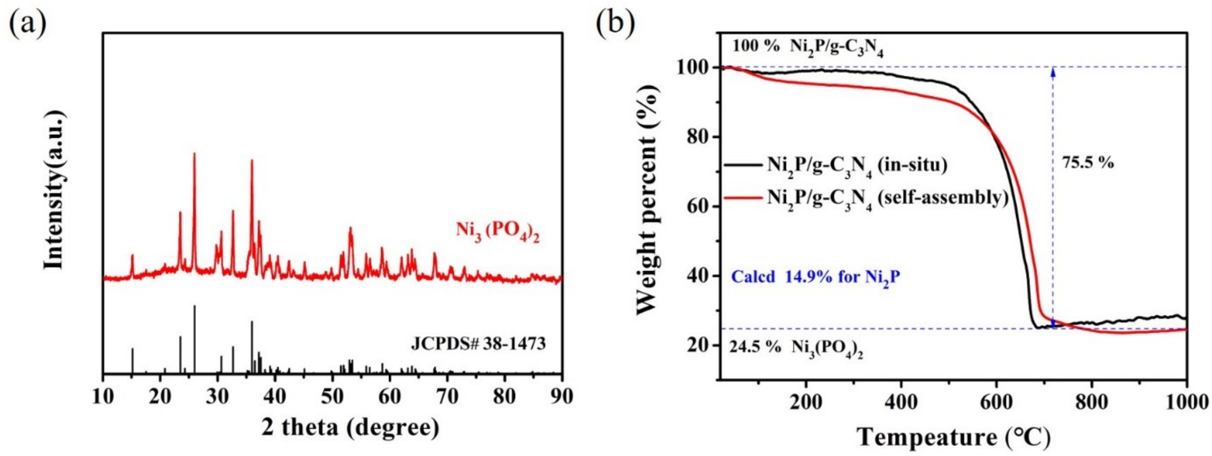

Fig. S9 (a) XRD pattern of the residue of Ni_2P/g-C_3N_4 composite after TGA measurement, (b) TGA curves of Ni_2P/g-C_3N_4 composite in flowing air atmospher

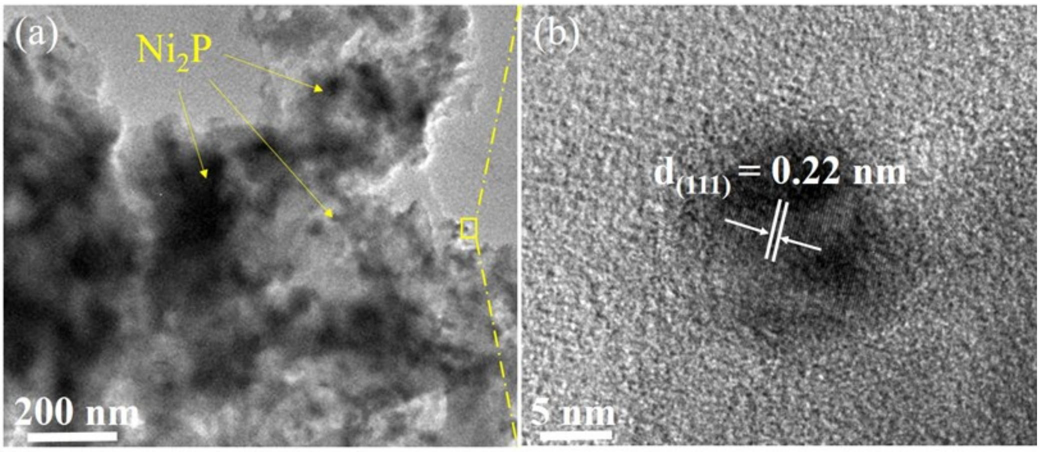

Fig. S10 (a) TEM and (b) HRTEM images of Ni_2P/g-C_3N_4 composite prepared by gas-solid method.

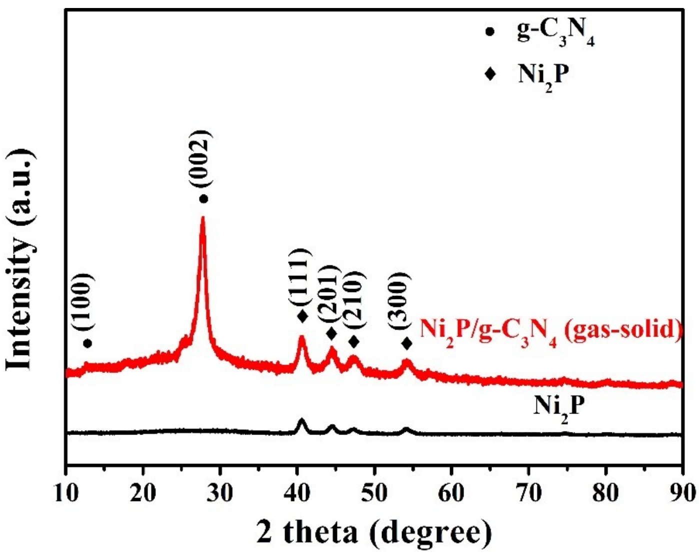

Fig. S11 XRD pattern of g-C_3N_4/Ni_2P composite prepared by gas-solid method.

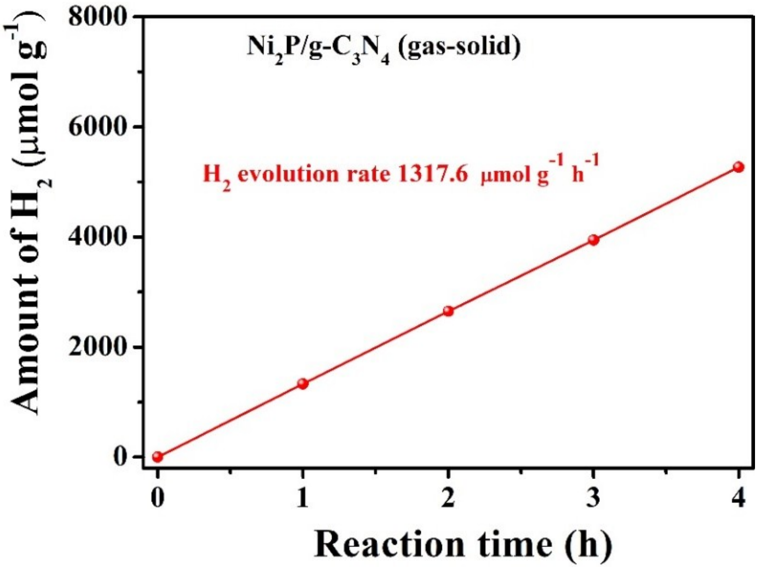

Fig. S12 Time-dependent overall water splitting over $Ni_2P/g\text{-}C_3N_4$ (gas-solid) sample in an aqueous solution of TEOA (10 vol%, 100 mL). A 300 W Xenon arc lamp (Newport) equipped with a UV-off filter ($\lambda > 420$ nm) was applied as the visible light source.

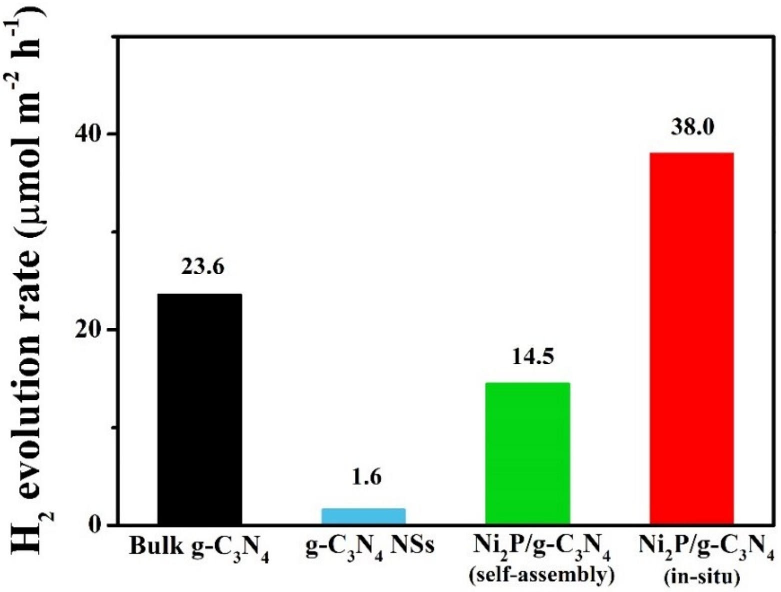

Fig. S13 H_2 evolution rate related to the BET specific surface area of bulk $g\text{-}C_3N_4$, $g\text{-}C_3N_4$ nanosheets, $Ni_2P/g\text{-}C_3N_4$ (self-assembly), and $Ni_2P/g\text{-}C_3N_4$ (in-situ) samples.

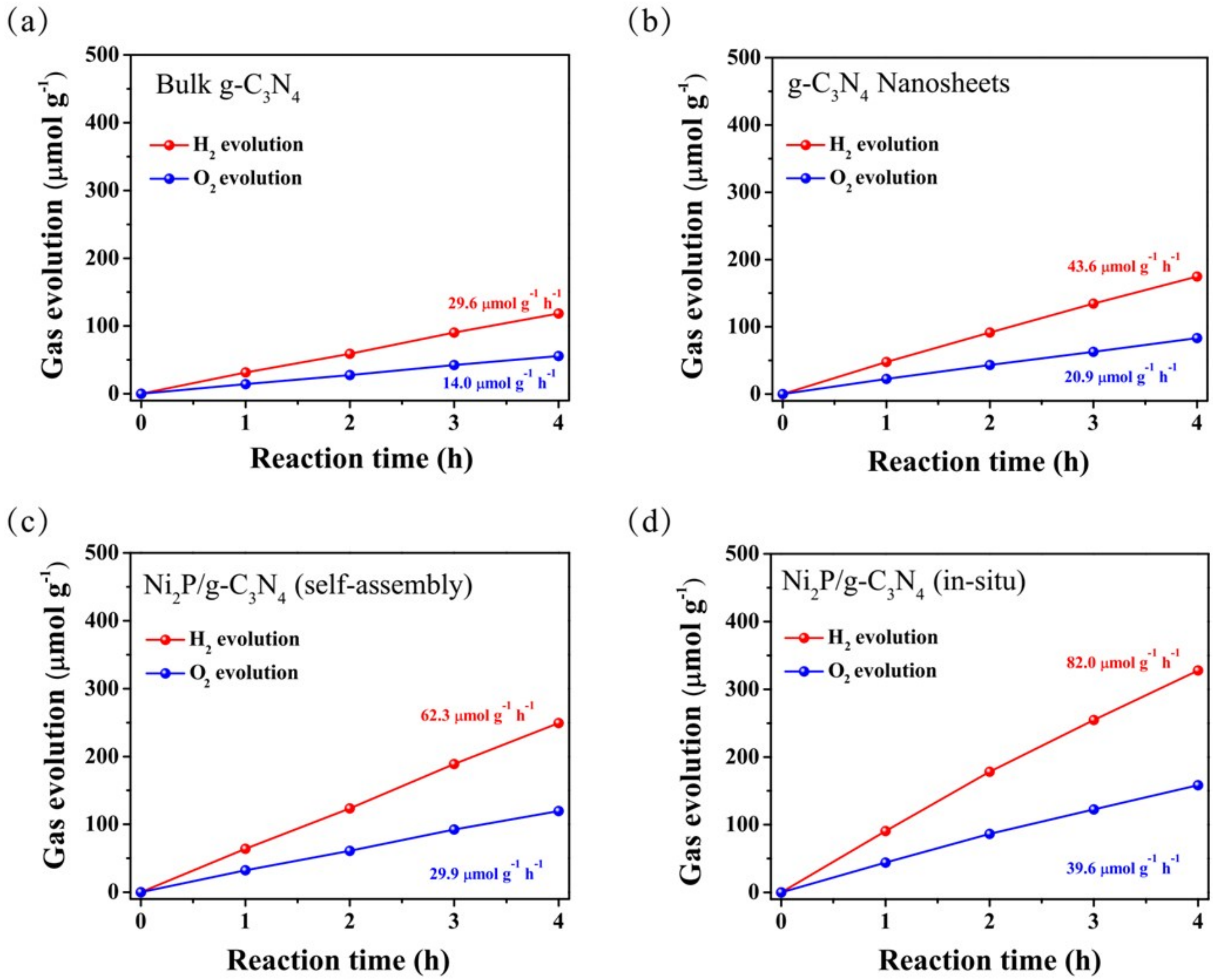

Fig. S14 Time-dependent overall water splitting over (a) bulk g-C_3N_4, (b) g-C_3N_4 NSs, (c) Ni_2P/g-C_3N_4 (self-assembly) and (d) Ni_2P/g-C_3N_4 (in-situ) in ultrapure water without sacrificial agent under visible light irradiation (λ>420 nm).

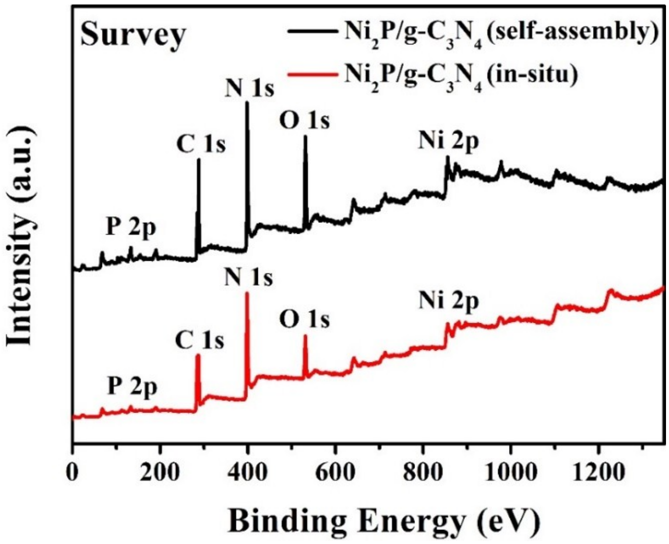

Fig. S15 XPS survey spectra of $Ni_2P/g\text{-}C_3N_4$ (self-assembly) and $Ni_2P/g\text{-}C_3N_4$ (in-situ) samples.

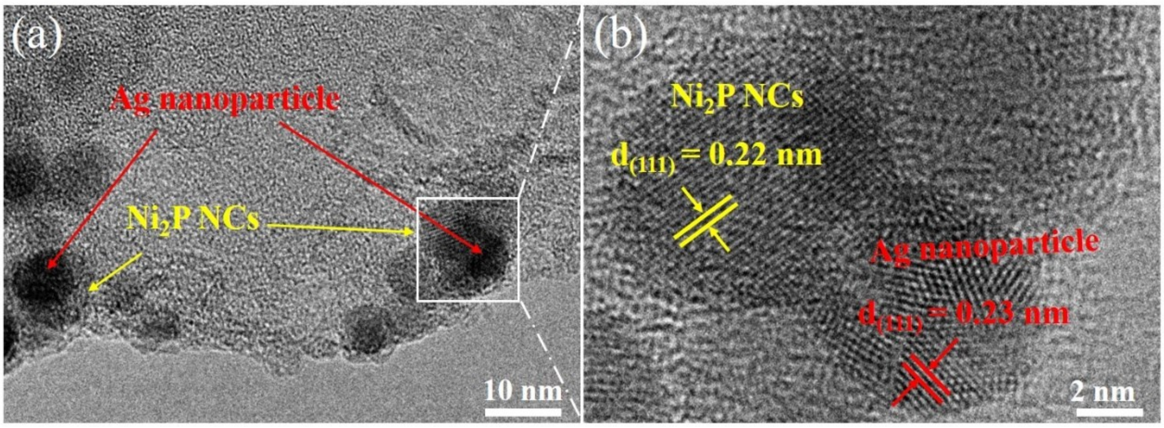

Fig. S16 (a) TEM image and (b) HRTEM image of the $Ni_2P/g\text{-}C_3N_4$ composite after water splitting experiment in 1 mM L^{-1} $AgNO_3$ aqueous solution under visible-light irradiation.

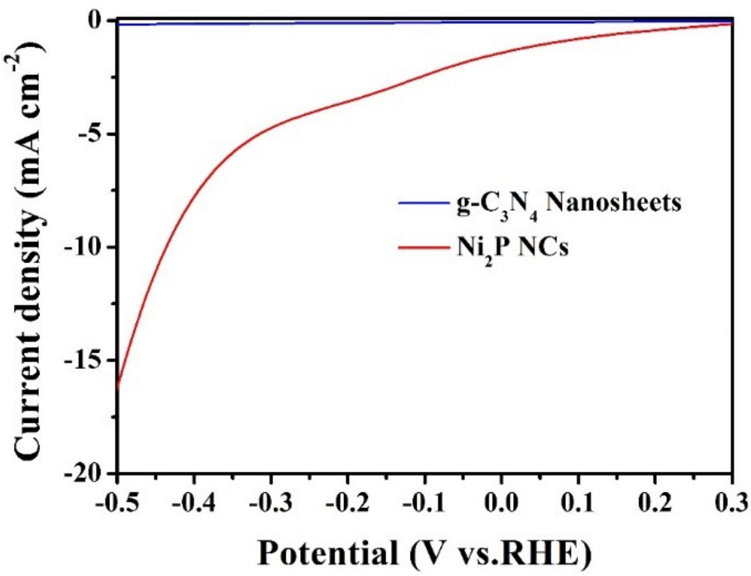

Fig. S17 Linear sweep voltammetry curves of $g\text{-}C_3N_4$ nanosheets and Ni_2P NCs in 0.1 M Na_2SO_4 aqueoussolution.

Table S3 Comparison of the photocatalytic H_2 generation performance of the g-C_3N_4-based systems loaded with non-noble-metal co-catalysts.

Catalyst	**Sacrificial reagent**	**Light source**	**Activity**	**Stability**	**AQY**	**Ref. (year)**
$MoSe_2$/g-C_3N_4	TEOA	300 W Xe lamp (λ> 420 nm)	136.8 μmol h^{-1} g^{-1}	>12 h	N/A	Reference S1 (2018)
$Ni_{12}P_5$/g-C_3N_4	TEOA	300 W Xe lamp (λ> 420 nm)	535.7 μmol h^{-1} g^{-1}	>30 h	4.67%（420 nm）	Reference S2 (2017)
0.5% Ni-1.0% NiS/g-C_3N_4	TEOA	300 W Xe lamp (λ> 420 nm)	515 μmol h^{-1} g^{-1}	>12 h	N/A	Reference S3 (2017)
NiS/g-C_3N_4	TEOA	300 W Xe lamp (λ> 420 nm)	16400 μmol h^{-1} g^{-1}	>40 h	N/A	Reference S4 (2018)
CoP/g-C_3N_4	TEOA	300 W Xe lamp (λ> 420 nm)	956.8 μmol h^{-1} g^{-1}	>70 h	3.65%（420 nm）	Reference S5 (2018)
FeP/g-C_3N_4	TEOA	300 W Xe lamp (λ> 420 nm)	177.9 μmol h^{-1} g^{-1}	>9 h	1.57%（420 nm）	Reference S6 (2019)
MoP/g-C_3N_4	TEOA	300 W Xe lamp (λ> 420 nm)	40.38 μmol h^{-1}	>15 h	18.3%（420 nm）	Reference S7 (2019)
MoS_2/g-C_3N_4	Methanol	300 W Xe lamp (λ> 420 nm)	577 μmol h^{-1} g^{-1}	>12 h	N/A	Reference S8 (2018)
Co_2P-K_2HPO_4/g-C_3N_4	TEOA	300 W Xe lamp	27.81 μmol h^{-1}	>15 h	N/A	Reference S9 (2017)
CoP/g-C_3N_4	TEOA	300 W Xe lamp (λ> 420 nm)	96.2 μmol h^{-1}	>12 h	12.4%（420 nm）	Reference S10 (2017)
Ni_3C/g-C_3N_4	TEOA	300 W Xe lamp (λ> 420 nm)	15.18 μmol h^{-1}	>12 h	0.4%（420 nm）	Reference S11 (2018)
Pt/g-C_3N_4	TEOA	300 W Xe lamp	318 μmol h^{-1}	>16 h	N/A	Reference S12 (2016)
Ni_2P/g-C_3N_4	**TEOA**	**300 W Xe lamp (λ> 420 nm)**	**2849.5 μmol h^{-1} g^{-1}**	**>20 h**	**18.8%（420 nm）**	**This Work**

Table S4 EXAFS fitting parameters corresponding to the fit for as-prepared samples in **Fig.S5** b.

Sample	**Shell**	**CN**	**R (Å)**	**σ^2 (10^{-3} Å^2)**
Ni_2P/g-C_3N_4 (in-situ)	Ni-Ni	2.24 ± 0.03	2.85 ± 0.01	6.4 ± 0.7
	Ni-P	2.18 ± 0.02	2.25 ± 0.01	5.4 ± 0.5
	Ni-N	1.75 ± 0.03	1.88 ± 0.02	5.8 ± 0.8
Ni_2P/g-C_3N_4 (self-assemble)	Ni-Ni	2.54 ± 0.02	2.81 ± 0.03	4.7 ± 0.6
	Ni-P	2.43 ± 0.04	2.19 ± 0.02	5.9 ± 0.5
Ni_2P Powder	Ni-Ni	2.46 ± 0.03	2.88 ± 0.02	6.4 ± 0.6
	Ni-P	2.38 ± 0.02	2.20 ± 0.01	7.3 ± 1.0
Ni foil	Ni-Ni	12.0	2.88 ± 0.03	5.8 ± 0.3

CN is the coordination number; R is interatomic distance (the bond length between Ni central atoms and surrounding coordination atoms); σ^2 is Debye-Waller factor (a measure of thermal and static disorder in absorber-scatter distances).

Table S5 Exponential decay-fitted parameters of fluorescence lifetime for bulk g-C_3N_4, g-C_3N_4 nanosheets, Ni_2P/g-C_3N_4 (in-situ), and Ni_2P/g-C_3N_4 (self-assembly) samples.

Samples	**A_1 (%)**	**τ_1 (ns)**	**A_2 (%)**	**τ_2 (ns)**	**τ_{ave} (ns)**
Bulk g-C_3N_4	35.70	2.5647	64.3	9.8071	8.89
g-C_3N_4 Nanosheets	33.21	2.4804	66.79	8.4798	7.72
Ni_2P/g-C_3N_4 (self-assembly)	46.58	2.2417	53.42	8.3902	7.23
Ni_2P/g-C_3N_4 (in-situ)	52.11	1.9637	47.89	7.9579	6.69

Table S6 Corresponding resistance of bulk g-C_3N_4, g-C_3N_4 nanosheets, Ni_2P/g-C_3N_4 (self-assembly), and Ni_2P/g-C_3N_4 (in-situ) samples.

Photocatalysts	**R_s/Ohm**	**$R_{ct}/10^5$ Ohm**
Bulk g-C_3N_4	60.9	13.77
g-C_3N_4 Nanosheets	57.3	9.51
Ni_2P/g-C_3N_4 (self-assembly)	56.11	3.36
Ni_2P/g-C_3N_4 (in-situ)	55.44	2.58

References

S1 D. Zeng, P. Wu, W.-J. Ong, B. Tang, M. Wu, H. Zheng, Y. Chen and D.-L. Peng, *Appl. Catal., B,* 2018, 233, 26-34.

S2 D. Zeng, W.-J. Ong, H. Zheng, M. Wu, Y. Chen, D.-L. Peng and M.-Y. Han, *J. Mater. Chem. A,* 2017, 5, 16171-16178.

S3 J. Wen, J. Xie, H. Zhang, A. Zhang, Y. Liu, X. Chen and X. Li, *ACS Appl. Mater. Interfaces*, 2017, 9, 14031-14042.

S4 H. Zhao, H. Zhang, G. Cui, Y. Dong, G. Wang, P. Jiang, X. Wu and N. Zhao, *Appl. Catal., B,* 2018, 225, 284-290.

S5 F. Zhang, J. Zhang, J. Li, X. Jin, Y. Li, M. Wu, X. Kang, T. Hu, X. Wang, W. Ren and G. Zhang, *J. Mater. Chem. A,* 2019, 7, 6939-6945.

S6 D. Zeng, T. Zhou, W. J. Ong, M. Wu, X. Duan, W. Xu, Y. Chen, Y. A. Zhu and D. L. Peng, *ACS Appl. Mater. Interfaces*, 2019, 11, 5651-5660.

S7 J.-Y. Tang, D. Yang, W.-G. Zhou, R.-T. Guo, W.-G. Pan and C.-Y. Huang, *J. Catal.*, 2019, 370, 79-87.

S8 Y. Liu, H. Zhang, J. Ke, J. Zhang, W. Tian, X. Xu, X. Duan, H. Sun, M. O Tade and S. Wang, *Appl. Catal., B,* 2018, 228, 64-74.

S9 R. Shen, J. Xie, H. Zhang, A. Zhang, X. Chen and X. Li, *ACS Sustain. Chem. Eng.*, 2017, 6, 816-826.

S10 C. Li, Y. Du, D. Wang, S. Yin, W. Tu, Z. Chen, M. Kraft, G. Chen and R. Xu, *Adv. Funct. Mater.*, 2017, 27.

S11 K. He, J. Xie, Z.-Q. Liu, N. Li, X. Chen, J. Hu and X. Li, *J. Mater. Chem. A,* 2018, 6, 13110-13122.

S12 X. Li, W. Bi, L. Zhang, S. Tao, W. Chu, Q. Zhang, Y. Luo, C. Wu and Y. Xie, *Adv Mater*, 2016, 28, 2427-2431.